






Article

# 1-Benzyl-5-bromo-3-hydrazonoindolin-2-ones as Novel Anticancer Agents: Synthesis, Biological Evaluation and Molecular Modeling Insights

Tarfah Al-Warhi <sup>1</sup>, Hadia Almahli <sup>2</sup>, Raed M. Maklad <sup>3</sup> , Zainab M. Elsayed <sup>4</sup>, Mahmoud A. El Hassab <sup>5</sup> , Ohoud J. Alotaibi <sup>1</sup>, Nada Aljaeed <sup>1</sup>, Rezk R. Ayyad <sup>6</sup>, Hazem A. Ghabour <sup>7</sup> , Wagdy M. Eldehna <sup>3,8,\*</sup> , and Mohamed K. El-Ashrey <sup>9</sup> 

- <sup>1</sup> Department of Chemistry, College of Science, Princess Nourah Bint Abdulrahman University, P.O. Box 84428, Riyadh 11671, Saudi Arabia
  - <sup>2</sup> Department of Chemistry, University of Cambridge, Cambridge CB2 1EW, UK
  - <sup>3</sup> Department of Pharmaceutical Chemistry, Faculty of Pharmacy, Kafrelsheikh University, Kafrelsheikh 33516, Egypt
  - <sup>4</sup> Scientific Research and Innovation Support Unit, Faculty of Pharmacy, Kafrelsheikh University, Kafrelsheikh 33516, Egypt
  - <sup>5</sup> Department of Medicinal Chemistry, Faculty of Pharmacy, King Salman International University (KSIU), South Sinai 46612, Egypt
  - <sup>6</sup> Department of Pharmaceutical Chemistry, Faculty of Pharmacy, Al-Azhar University, Cairo 11884, Egypt
  - <sup>7</sup> Department of Medicinal Chemistry, Faculty of Pharmacy, Mansoura University, Mansoura 35516, Egypt
  - <sup>8</sup> School of Biotechnology, Badr University in Cairo, Badr City 11829, Egypt
  - <sup>9</sup> Pharmaceutical Chemistry Department, Faculty of Pharmacy, Cairo University, Kasr Elini St., Cairo 11562, Egypt
- \* Correspondence: wagdy2000@gmail.com



**Citation:** Al-Warhi, T.; Almahli, H.; Maklad, R.M.; Elsayed, Z.M.; El Hassab, M.A.; Alotaibi, O.J.; Aljaeed, N.; Ayyad, R.R.; Ghabour, H.A.; Eldehna, W.M.; et al. 1-Benzyl-5-bromo-3-hydrazonoindolin-2-ones as Novel Anticancer Agents: Synthesis, Biological Evaluation and Molecular Modeling Insights. *Molecules* **2023**, *28*, 3203. <https://doi.org/10.3390/molecules28073203>

Academic Editor: Ines Bruno

Received: 1 March 2023

Revised: 24 March 2023

Accepted: 26 March 2023

Published: 4 April 2023



**Copyright:** © 2023 by the authors. Licensee MDPI, Basel, Switzerland. This article is an open access article distributed under the terms and conditions of the Creative Commons Attribution (CC BY) license (<https://creativecommons.org/licenses/by/4.0/>).

**Abstract:** Human health is experiencing several obstacles in the modern medical era, particularly cancer. As a result, the cancer therapeutic arsenal should be continually expanded with innovative small molecules that preferentially target tumour cells. In this study, we describe the development of two small molecule series (**7a–d** and **12a–e**) based on the 1-benzyl-5-bromoindolin-2-one scaffold that connected through a hydrazone linker to a 4-arylthiazole (**7a–d**) or 4-methyl-5-(aryldiazenyl)thiazole (**12a–e**) moiety. The anticancer activity of all the reported indolin-2-one derivatives was assessed against breast (MCF-7) and lung (A-549) cancer cell lines. The 4-arylthiazole-bearing derivatives **7c** and **7d** revealed the best anticancer activity toward MCF-7 cells ( $IC_{50} = 7.17 \pm 0.94$  and  $2.93 \pm 0.47$ , respectively). Furthermore, the VEGFR-2 inhibitory activity for **7c** and **7d** was evaluated. Both molecules disclosed good inhibitory activity, and their  $IC_{50}$  values were equal to  $0.728 \mu\text{M}$  and  $0.503 \mu\text{M}$ , respectively. Additionally, the impacts of **7d** on the cell cycle phases as well as on the levels of different apoptotic markers (caspase-3, caspase-9, Bax, and Bcl-2) were assessed. Molecular docking and dynamic simulations are carried out to explore the binding mode of **7d** within the VEGFR-2 active site.

**Keywords:** thiazole; anti-proliferative; isatin; MCF-7 cells; A-549 cells; VEGFR-2 inhibitor; molecular dynamics

## 1. Introduction

Numerous obstacles face human health in the modern medical era, particularly cancer [1]. Therefore, new small compounds should continuously be added to the treatment toolbox for cancer to specifically target tumour cells while posing little risk of damage to normal cells [2–9].

Angiogenesis is a complicated process that, under both physiological and pathological situations, is regulated by the creation of a wide variety of pro- and anti-angiogenic factors.

Different diseases, such as rheumatoid arthritis, age-related macular degeneration, diabetic retinopathy, atherosclerosis, and cancer, have, however, been linked to an imbalance between these factors that govern angiogenesis [10]. Malignant cells must be substantially vascularized to get more oxygen and nutrients to survive and grow, making angiogenesis a crucial process. It was evidenced that the VEGF/VEGFR-2 signalling pathway stimulates several endothelial responses with a noticeable ability to increase the permeability of vessels and enhance the proliferation, differentiation, and migration of the cancerous endothelial cells [11,12]. As a result, the avoidance of angiogenesis through the suppression of VEGFR-2 could be a very effective cancer-fighting tactic [10].

The isatin motif has surfaced as a privileged scaffold with numerous and significant pharmacological actions [13], such as antimicrobial [14], antiviral [15], and anticancer [16] effects. Noteworthy, isatin moiety has been included in some clinically approved medications such as Nintedanib and Sunitinib (Figure 1). As an important approach in drug design and discovery [17], several research studies have exploited the hybridization approach to develop diverse isatin-based conjugates as effective anticancer agents [18–20]. For instance, pyridine [21], azole [22], coumarin [23], thiazolo [3,2-*a*] benzimidazole [24], benzofuran [25,26], phthalazine [27], quinazoline [28], indole [29,30], thiazolidinone [31], and oxadiazole [32]. Additionally, it is worth mentioning that several studies have presented the isatin motif as a privileged scaffold for the development of diverse small molecule sets with significant kinase inhibitory activities [33].

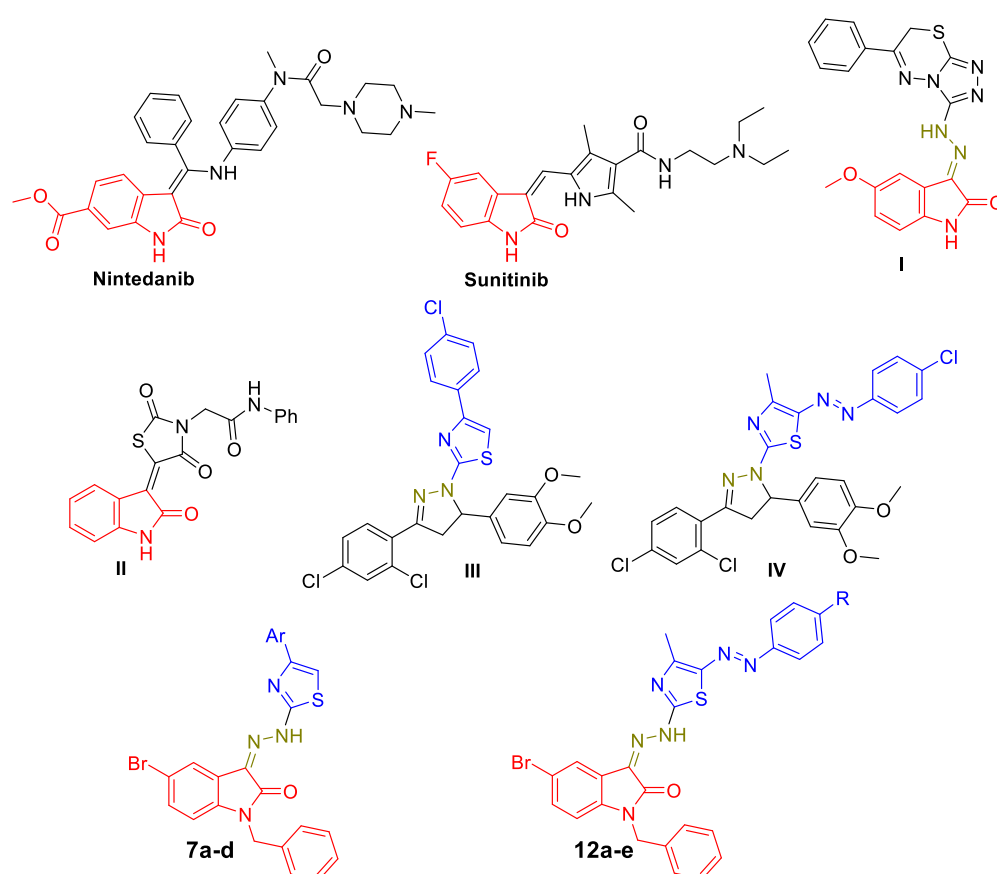


**Figure 1.** Structure of Nintedanib, Sunitinib, VEGFR-2 inhibitors (I–IV), and target molecules (7a–d and 12a–e).

After the FDA's approval of the VEGFR-2 inhibitor Sunitinib, medicinal chemists have paid special attention to the identification of new isatin-based anti-cancer candidates targeting VEGFR-2 kinase [32–44]. Our research team has recently reported several VEGFR-2 inhibitors based on the isatin scaffold [45–50]. In 2020, we developed a new

set of triazolo[3,4-*b*]thiadiazine—isatin hybrids with promising anti-angiogenic activities [46]. Compound **I** (Figure 1) disclosed broad antitumour activities in the NCI-USA anticancer assay (growth inhibition mean = 40%), along with good VEGFR-2 inhibition ( $IC_{50}$  = 435 nM). Moreover, the angiogenesis HET-CAM assay was used to check the mortality and toxicity of the target hybrids. Compound **I** remarkably reduced the developed blood vessels; in addition, it was not toxic for the chick embryos. In the last year, another small set of 2,4-thiazolidindione—isatin hybrids with promising anticancer and VEGFR-2 inhibitory activities were reported [47–49]. Compound **II** (Figure 1) revealed good anti-proliferative activities toward breast, lung, and colon cancer cell lines. Additionally, it exerted a potent inhibitory effect against VEGFR-2, with an  $IC_{50}$  of 84.05 nM.

On the other hand, another study has reported a series of pyrazoline derivatives decorated with 4-arylthiazole and 4-methyl-5-(aryldiazenyl)thiazole moieties as potent anticancer agents with an effective inhibitory effect against VEGFR-2. For example, compounds **III** and **IV** (Figure 1) displayed excellent cell growth inhibitory activity toward non-small lung cancer H441 and A549 cell lines, as well as good inhibitory activity against VEGFR-2 ( $IC_{50}$  = 185.5 nM and 113.3 nM, respectively) [50].

Utilizing the aforementioned findings, this article describes the development of two small molecule series (**7a–d** and **12a–e**) based on the 1-benzyl-5-bromoindolin-2-one scaffold that connected through a hydrazone linker to a 4-arylthiazole (**7a–d**) or 4-methyl-5-(aryldiazenyl)thiazole (**12a–e**) moiety. The anticancer activity for all the reported indolin-2-one derivatives was assessed against the VEGFR-2-overexpressing breast (MCF-7) and lung (A-549) cancer cell lines. Thereafter, the VEGFR-2 inhibitory activity was evaluated for the best anti-proliferative molecules. Moreover, the impact of target compounds on the cell cycle phases as well as on the levels of different apoptotic markers (caspases-3, caspase-9, Bax, and Bcl-2) was assessed. Molecular docking and dynamic simulations were carried out to explore the binding mode within the VEGFR-2 active site.

## 2. Results and Discussion

### 2.1. Chemistry

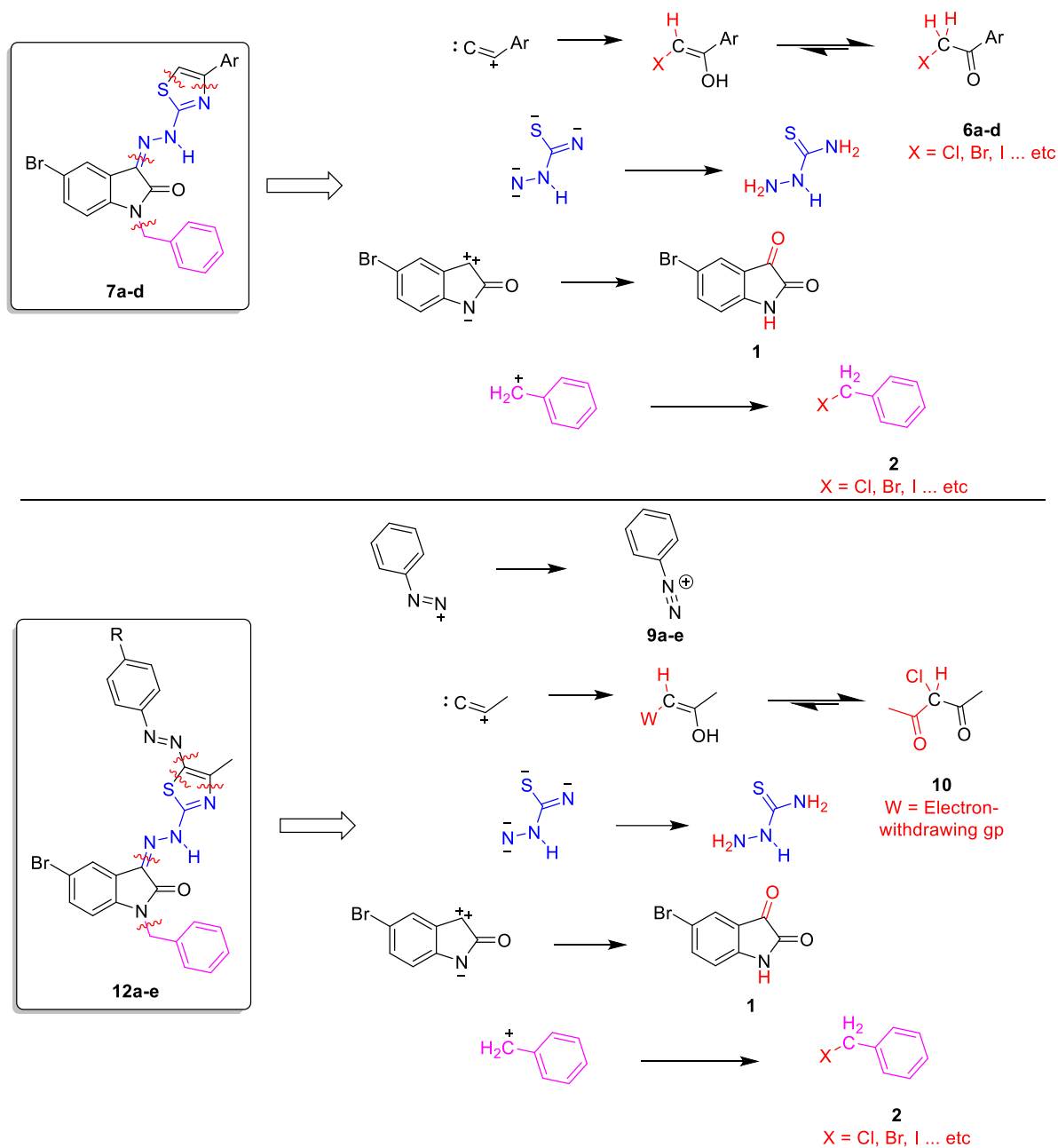
Target 1-benzyl-5-bromo-3-hydrazoneindolin-2-one derivatives **7a–d** and **12a–e** were subjected to retrosynthetic analysis to gain insights into potentially useful starting materials and chemical reagents to start their chemical syntheses (Scheme 1).

Upon applying the disconnection strategy to compounds **7a–d**, an aromatic  $\alpha$ -haloketone (**6**), thiosemicarbazide, an isatin derivative (**1**), and benzyl halide (**2**) molecules were obtained. The retrosynthesis of target compounds **12a–e** was not remarkably different, except for the phenylazo moiety, which has inspired us with a diazonium salt (**9**), in addition to the aliphatic ketone (**10**) starting materials (Scheme 2).

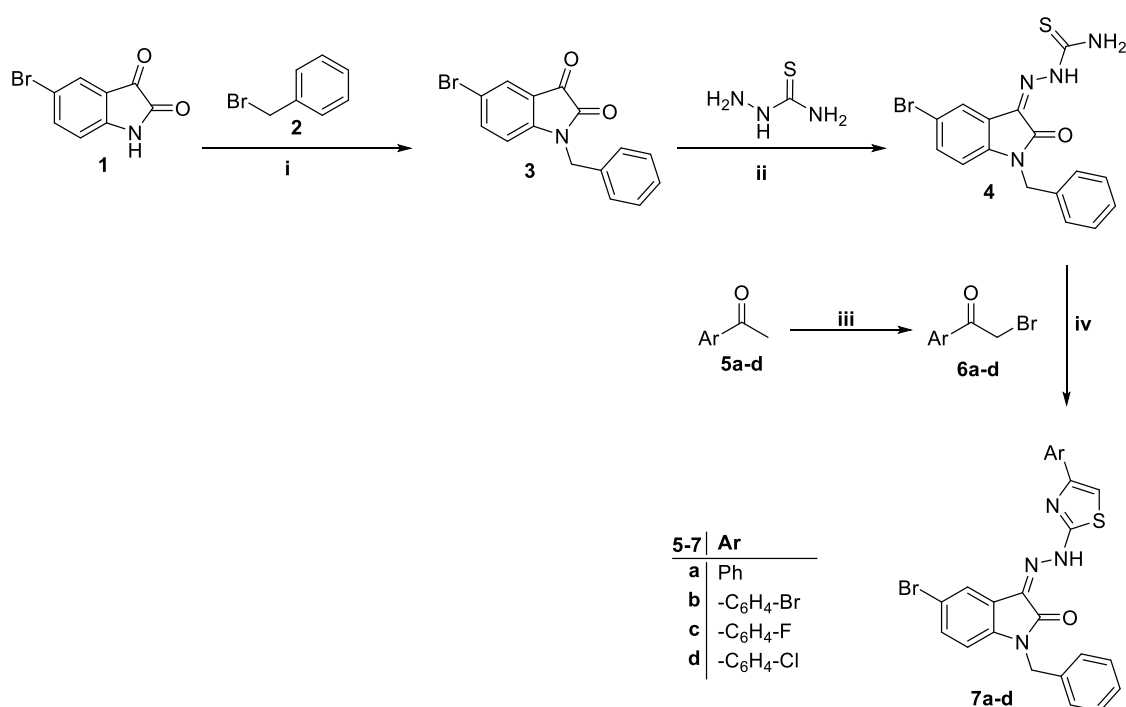
Accordingly, *N*-benzylisatin derivative (**3**) was prepared by a nucleophilic substitution reaction of benzyl bromide (**2**) with isatin derivative (**1**) under  $S_N2$  reaction conditions, namely in a basic medium (anhydrous potassium carbonate) in a polar aprotic solvent (acetonitrile), as shown in Scheme 2. Then, the ketonic carbonyl group of compound (**3**) underwent a condensation reaction with thiosemicarbazide to furnish a thiosemicarbazone derivative (**4**, Scheme 2).

On the other hand, aromatic ketones (**5a–d**) were subjected to straightforward  $\alpha$ -bromination using cupric bromide ( $Cu_2Br$ ) in a refluxing chloroform/ethyl acetate (1:1) solvent mixture following the reported method [51]. This afforded the ambident electrophilic reagents (**6a–d**) needed for the next step (Scheme 2) through a straightforward alternative route to the NBS-based [52,53] C-H bromination. Thereafter, the bifunctional electrophilic reagents (**6a–d**) were allowed to react with the ambident nucleophilic thiosemicarbazone substrate (**4**), affording the targeted thiazol-2-ylhydrazineylideneisatin derivatives **7a–d** (Scheme 2). The reaction involved regioselective [3+2] 4-substitutedthiazole ring cyclization in which the softer electrophilic motif ( $\alpha$ -bromo Csp<sup>3</sup>) preferentially reacts with the softer nucleophilic one (sulfur) and the harder electrophilic one (ketonic carbonyl group) selectively reacts with the harder nucleophilic one ( $NH_2$ ). Although the *N*-alkylation reac-

tions of nitrogen-based nucleophiles with  $\alpha$ -halo carbonyl compounds are common [54,55], the issue discussed herein only represents a matter of competition between sulfur- and nitrogen-based nucleophilic sites for the electrophile. Analogous regioselectivity of similar cyclization reactions [22] and theoretical aspects [56] of the Hard and Soft Acid and Base Theory (HSABT) have been previously discussed elsewhere. It is of special interest to mention the ease with which the thiazole cyclization reaction took place even with neither acid nor base catalysis. This may be due to the high reactivity of the ketonic C=O (in series 6) as compared to the relatively less reactive C=O of the ester analogues in similar reactions (which impose base catalysis, e.g., with NaOAc).



**Scheme 1.** Retrosynthesis of target compounds 7a–d and 12a–e.



**Scheme 2.** Reagents and conditions: (i) Anhydrous  $K_2CO_3$ , MeCN, r.t, 12 h; (ii) EtOH, cat. HOAc (a few drops), reflux 5 h; (iii)  $CuBr_2$  (2 equiv.),  $CHCl_3$ /EtOAc 1:1, reflux 4 h; (iv) Absolute EtOH, reflux 7 h.

Analogously, target compounds **12a–e** (Scheme 3) were best obtained by considering the reagents and starting substrates inspired by their retrosynthetic analysis (shown in Scheme 1). Firstly, diazotization of anilines (**8a–e**) at 0 °C afforded the desired diazonium salts (**9a–e**), which were utilised as aqueous solutions in the next step. As for the azo-coupling reaction, it is considered a highly useful synthetic route to biologically active molecules [57]. More specifically, there is a possible disconnection route for the preparation of target compounds (**12a–e**) through azo-coupling of diazonium salts (e.g., **9a–e**) with thiazole scaffolds, which are prepared by reacting thiosemicarbazones (e.g., **4**) with 3-chloroacetylacetone (**10**) [58], where the coupling reaction took place at thiazole C5 [59]. Nevertheless, the current study considered the Japp-Klingemann pathway, which utilised a more favoured azo-coupling with an enolate ion.

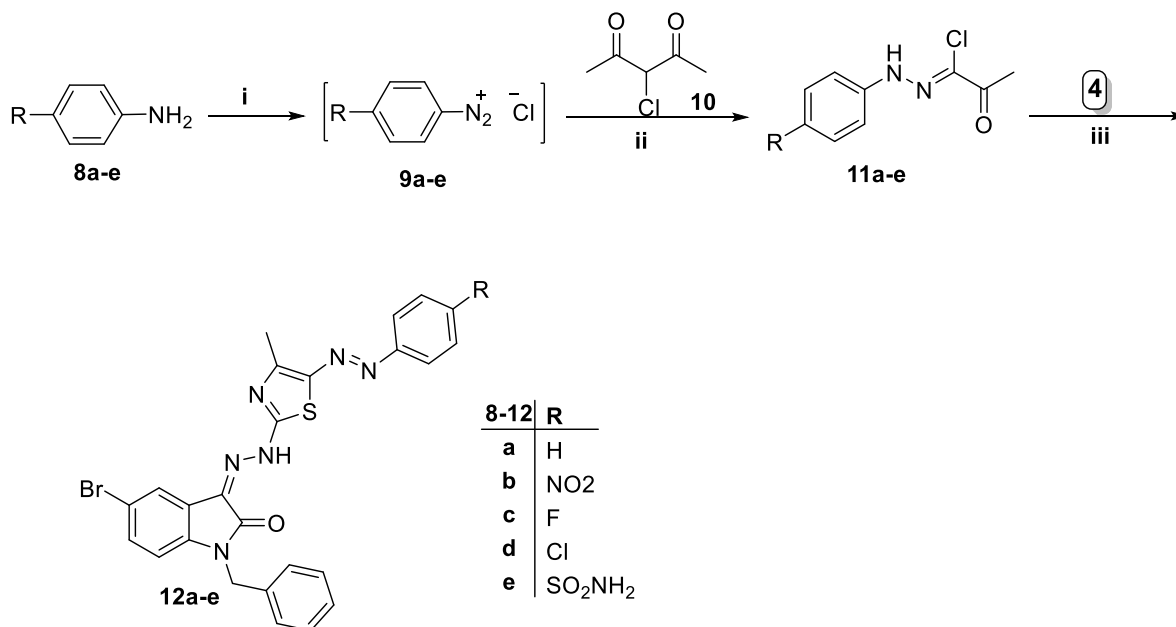
Accordingly, the enolate anion of 3-chloroacetylacetone (prepared in situ by treatment of the latter with sodium acetate) was subjected to nucleophilic addition to the diazonium salt series (**9a–e**) via the Japp-Klingemann reaction [60] to afford the corresponding hydrazonoyl chlorides **11a–e** (Scheme 3).

After that, target 5-(phenylazo)thiazol-2-ylhydrazineylideneisatin derivatives (**12a–e**) were finally obtained by regioselective [3+2] thiazole ring cyclization, which was closely related to what has been discussed earlier regarding the last step in Scheme 2.

Although similar reactions were reported involving thiosemicarbazones derived from aromatic aldehydes or ketones, the analogous isatin-3-ylidene thiosemicarbazones were rarely studied. To the best of our knowledge, this is the second research work addressing the isatin-3-ylidene thiosemicarbazone motif reacting with hydrazonoyl chlorides obtained via the Japp-Klingemann pathway [61].

Furthermore, the reaction mechanism deserves much consideration, both in terms of the electrophilic species and the final cyclization step. Although the detailed evidence-based mechanistic study is beyond the scope of this article, it is noteworthy for reporting some relevant and controversial issues. In a few studies, it is suggested that the first step is a nucleophilic substitution of halide by sulphur (mostly by addition–elimination to  $C=N$ ) [62,63]. This is while an alternative possibility of a nitrilimine intermediate (e.g.,

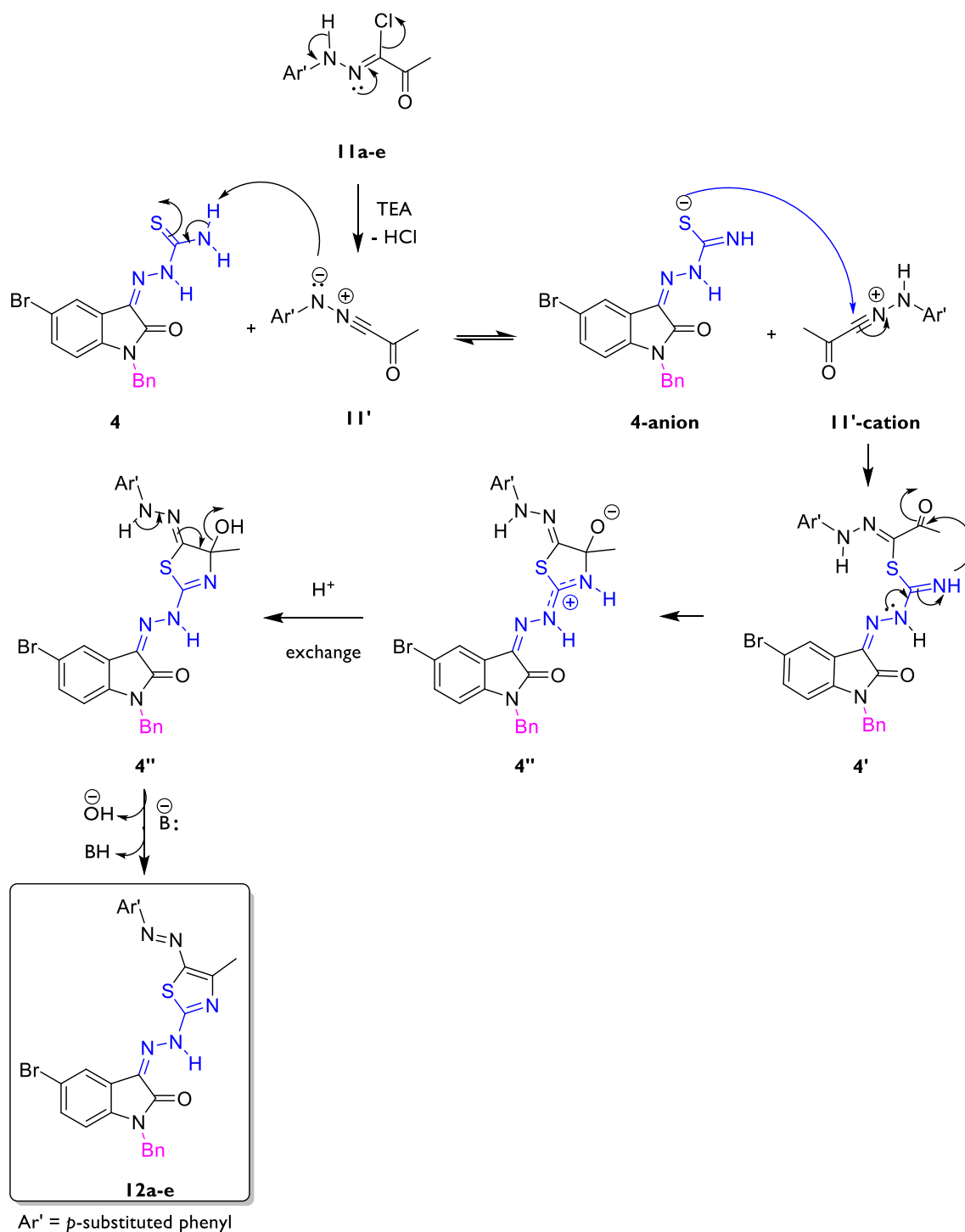
**11'**, Scheme 4) (whose existence was supported by X-ray-assisted DFT study alongside other experimental evidence in cycloaddition reactions and those involving hydrazonoyl chlorides in basic media [64,65]) still stands as a challenging one in the thiazole cyclization discussed herein (Scheme 4). Accordingly, the existence of nitrilimine (**11'**) was safely suggested herein upon the action of triethylamine on hydrazonoyl chlorides (**11a–e**) as in Scheme 4.



**Scheme 3.** Reagents and conditions: (i) HCl 37% (2.5 equiv.), NaNO<sub>2</sub> (1.1 equiv. added dropwise), dist. water, ice bath 0 °C, 30 min; (ii) NaOAc, EtOH/water, ice bath 0 °C, 2 h; (iii) Dioxane, TEA, reflux 5 h.

Furthermore, an acid-base equilibrium was suggested to take place in which the nitrilimine (**11'**) would act as a base that abstracts the relatively acidic NH proton of thiosemicarbazone (**4**). This equilibrium furnishes considerable concentrations of the activated electrophilic nitrilium-ion form of the former (**11'-cation**) alongside the activated nucleophilic anion form of the latter (**4-anion**), as outlined in Scheme 4. These equilibrium concentrations would be fairly sufficient for the next nucleophilic addition of the **4-anion** to the C-N triple bond of the nitrilium ion (**11'-cation**) to produce the open-chain hydrazonoyl thiolate intermediate (**4'**). Further intramolecular nucleophilic cycloaddition and subsequent tautomerism would afford the thiazolidine derivative (**4''**), which would finally be driven to approach aromaticity by elimination of the water molecule to afford the desired thiazole derivatives (**12a–e**), see Scheme 4.

Finally, the chemical structures of target compounds **7a–d** and **12a–e** were confirmed by NMR spectroscopic analyses. The coexistence of the aromatic proton signals relevant to the isatin-3-ylidene, benzyl, and 4-methylthiazolyl moieties, showing the proper integrals for each, afforded strong evidence confirming the series **7a–d**. Additional aromatic proton signals of the phenylazo moiety showing the expected integral values provided evidence for confirming the structures of the series **12a–e**. It is noteworthy that according to the <sup>1</sup>H NMR spectra, the target *N*-benzyl-5-bromoindolin-2-one derivatives exist as *E*- and *Z*-isomers. However, they interconvert rapidly in solution at room temperature and cannot be separated. Generally, the ratios of such indolinone hydrazone isomers are solvent- and temperature-dependent, as previously reported [66–68]. Thus, these isomers are not separable. We have reported several isatin hydrazone series that afford an *E/Z* mixture [25,27,69,70]. Further details are available in the “Experimental” section.

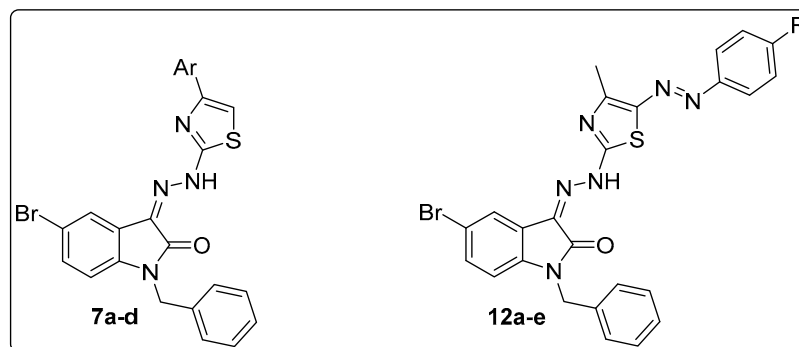


**Scheme 4.** Suggested mechanism of the base-catalyzed 4-substituted thiazole cyclization reaction of hydrazoneyl chlorides (**11a–e**) with thiosemicarbazone (**4**) to afford target compounds (**12a–e**).

## 2.2. Biological Evaluation

### 2.2.1. In Vitro Anti-Proliferative Activity

The anti-proliferative effect of the newly prepared *N*-benzyl-5-bromoindolin-2-one derivatives **7a–d** and **12a–e** was assessed in two human tumour cell lines: A-549 lung cancer and MCF-7 breast cancer. As a reference antitumour drug, doxorubicin was exploited in this experiment. The findings were expressed as median growth inhibitory concentration (IC<sub>50</sub>) values (Table 1).

**Table 1.** In vitro anticancer activities ( $IC_{50}$ ) for the synthesised *N*-benzyl-5-bromoindolin-2-one derivatives **7a–d** and **12a–e** against MCF-7 and A-549 cell lines.

Comd.	Ar/R	$IC_{50}$ ( $\mu M$ ) <sup>a</sup>	
		MCF-7	A-549
<b>7a</b>	C <sub>6</sub> H <sub>5</sub>	19.53 ± 1.05	NA <sup>b</sup>
<b>7b</b>	4-Br-C <sub>6</sub> H <sub>4</sub>	NA <sup>b</sup>	NA <sup>b</sup>
<b>7c</b>	4-F-C <sub>6</sub> H <sub>4</sub>	7.17 ± 0.94	20.43 ± 1.51
<b>7d</b>	4-Cl-C <sub>6</sub> H <sub>4</sub>	2.93 ± 0.47	9.57 ± 0.62
<b>12a</b>	H	39.53 ± 2.02	61.76 ± 4.01
<b>12b</b>	NO <sub>2</sub>	NA <sup>b</sup>	NA <sup>b</sup>
<b>12c</b>	F	27.65 ± 2.39	12.20 ± 1.54
<b>12d</b>	Cl	13.92 ± 1.21	29.45 ± 2.06
<b>12e</b>	SO <sub>2</sub> NH <sub>2</sub>	NA <sup>b</sup>	NA <sup>b</sup>
<b>Dox.</b>	-	4.30 ± 0.84	6.4 ± 0.79

<sup>a</sup>  $IC_{50}$  values are presented as means ± S.D. for 3 separate experiments. <sup>b</sup> NA:  $IC_{50}$  higher than 100  $\mu M$ .

As shown in Table 1, it is clear that a number of the prepared molecules had growth-inhibitory properties that ranged from good to modest for the examined tumour cell lines. Investigations into the anti-proliferative activity revealed that the MCF-7 cell line was more sensitive than the A-549 cell line to the effects of both series (**7a–d** and **12a–e**).

Concerning the growth inhibitory activity against MCF-7 cells, it is worth mentioning that the 4-arylthiazole bearing derivatives (**7a–d**) possessed better activity than their 4-methyl-5-(aryldiazenyl)thiazole analogous (**12a–e**). In particular, the 4-(*p*-chlorophenyl)thiazole bearing derivative **7d** ( $IC_{50} = 2.93 \pm 0.47 \mu M$ ) was the most potent counterpart with more enhanced activity than the reference drug doxorubicin ( $IC_{50} = 4.30 \pm 0.84 \mu M$ ). In addition, the 4-(*p*-fluorophenyl)thiazole bearing molecule **7c** showed good potency against MCF-7 cells ( $IC_{50} = 7.17 \pm 0.94 \mu M$ ). Furthermore, *N*-benzyl-5-bromoindolin-2-ones **7a** and **12d** were moderately potent toward MCF-7 cells, with  $IC_{50}$  values of  $19.53 \pm 1.05$  and  $13.92 \pm 1.21 \mu M$ , respectively. This is while compounds **12a** and **12c** exhibited weak anticancer potency towards MCF-7 cells ( $IC_{50} = 39.53 \pm 2.02$  and  $27.65 \pm 2.39 \mu M$ , respectively).

On the other hand, evaluation of the anticancer potency in A-549 cells revealed that both series did not display significant anti-proliferative activity, except compounds **7d** and **12c**, which showed moderate impact with  $IC_{50} = 9.57 \pm 0.62$  and  $12.20 \pm 1.54$ , respectively.

It is worth stressing that the decoration of the pendant phenyl motif in series **7** with a small (fluoride) or moderate (chloride) lipophilic substituent enhanced the anticancer potency towards MCF-7 cells. In detail, the *para*-substituted derivatives **7c–d** disclosed 2.7- and 5.6-fold more enhanced activity ( $IC_{50} = 7.17 \pm 0.94$  and  $2.93 \pm 0.47 \mu M$ , respectively) than their un-substituted analogue **7a** ( $IC_{50} = 19.53 \pm 1.05 \mu M$ ). On the contrary, grafting a large lipophilic substituent such as 4-Br into compound **7b** diminished the activity.

In a similar vein, the substitution of the pendant phenyl moiety in series **12** with 4-F or 4-Cl (compounds **12c** and **12d**;  $IC_{50} = 27.65 \pm 2.39$  and  $13.92 \pm 1.21 \mu M$ , respectively) improved the growth inhibitory potency towards lung A-549 cells concerning the unsubstituted derivative **12a** ( $IC_{50} = 39.53 \pm 2.02 \mu M$ ).



Furthermore, in this study, we assessed the potential cytotoxic effect of the best anti-proliferative *N*-benzyl-5-bromoindolin-2-one derivatives **7c** and **7d** on the non-tumourigenic breast MCF-10A cells. The results disclosed that both indolin-2-ones **7c** and **7d** have modest cytotoxic impacts against the examined normal cells, with IC<sub>50</sub> values of  $91.33 \pm 3.51 \mu\text{M}$  and  $83.04 \pm 4.10 \mu\text{M}$ , respectively.

### 2.2.2. VEGFR-2 Inhibition

In this work, the most powerful cytotoxic molecules towards the MCF-7 cell line (**7c** and **7d**) were chosen to be tested for their VEGFR-2 inhibitory function. The VEGFR-2 inhibitor sorafenib, which has been successfully approved, served as the study's reference medication. The findings were presented in the form of IC<sub>50</sub> values, which can be found in Table 1. According to the findings, the molecules **7c** and **7d** that were investigated possessed a level of VEGFR-2 inhibitory activity that was moderate. Their IC<sub>50</sub> values were equal to  $0.728 \mu\text{M}$  and  $0.503 \mu\text{M}$ , respectively (Table 2).

**Table 2.** IC<sub>50</sub> for the VEGFR-2 inhibitory action of **7c** and **7d**.

Compound	VEGFR-2 IC <sub>50</sub> (μM) <sup>a</sup>
<b>7c</b>	0.728
<b>7d</b>	0.503
<b>Sorafenib</b>	0.112

<sup>a</sup> IC<sub>50</sub> values are the mean  $\pm$  SD of three separate experiments.

### 2.2.3. Apoptosis Induction

The ability of cancer cells to stop apoptosis is directly linked to their ability to grow out of control. Thus, targeting apoptosis induction is an effective approach for preventing the growth of cancer cells [71,72]. In this study, we evaluated the apoptotic impact of **7d** as it proved to be the most active compound against the cell line MCF-7 (IC<sub>50</sub> =  $2.93 \pm 0.47 \mu\text{M}$ ) to investigate the effect of our compounds on the induction of the apoptotic cascade.

#### Effects on Activation of Proteolytic Caspases Cascade

The crucial apoptosis mediators are a family of cysteine-aspartic proteases known as caspases, whose activation has a significant impact on apoptosis induction [73]. Accordingly, the impact of 1-benzyl-5-bromoindolin-2-one derivative **7d** on caspase 3 was evaluated. Being the executioner caspase, its induction gives insight into the pro-apoptotic effect of **7d**. Moreover, the effect of **7d** on the activation of caspase-9 was determined for further evaluation of the pro-apoptotic activity.

Our results fathomed that **7d** induced the level of active caspase-3 by 18.3 fold as compared to the control, which implies its possession of significant pro-apoptotic activity. Furthermore, **7d** potentiated the level of active caspase-9 by 16.7 fold in comparison to the control. This implies that the intrinsic pathway was definitely adopted (Table 3).

**Table 3.** Effect of *N*-benzylindolin-2-one derivative **7d** on the active caspases-3 and -9 levels and the Bax and Bcl-2 expression levels in MCF-7 cells after treatment with **7d** at its IC<sub>50</sub> concentration.

Comp.	Caspase-3 IU/mL	Caspase-9 IU/mL	Bax IU/mL	Bcl-2 IU/mL	Bax/Bcl-2 Ratio
<b>Control</b>	0.0156	0.0111	1.3	3.137	0.4144
<b>7d</b>	0.2862 ***	0.1853 **	102.9 ***	0.6449 **	159.56

\*\* Significantly different from control at  $p < 0.01$ . \*\*\* Significantly different from control at  $p < 0.001$ .

#### Effects on Mitochondrial Apoptosis Pathway (Bcl-2 Family) Proteins

It is well established that the apoptotic switch on/off mechanism is precisely tuned by the Bcl-2 family of proteins, which are classified mainly into two classes: anti-apoptotic

proteins such as Bcl-2 protein and the counteracting pro-apoptotic proteins, including Bax protein [74]. Inhibition of class I proteins and/or the activation of class II proteins can successfully induce apoptosis. Using Bcl-2 as a representative member of class I and Bax as a representative member of class II, we assessed the impact of **7d** on their levels in the MCF-7 cells. Moreover, the ratio between both proteins was detected as a determining factor for cell death regulation (Table 3).

As revealed in Table 3, **7d** downregulated the level of Bcl-2 by 4.9 folds in comparison to the control, while it effectively boosted the Bax level by 79.2 folds as compared to the control. The Bax/Bcl-2 ratio is a rather more indicative and conclusive value that precisely estimates the apoptotic effect. Notably, **7d** boosted this ratio by 159.56 folds as compared to the control. Collectively, the upregulation of Bax, the increase in the ratio of Bax to Bcl-2, and the downregulation of Bcl-2 all pointed to the suggestion that compound **7d** has a pro-apoptotic effect.

#### 2.2.4. Cell Cycle Analysis

Cytotoxic agents abort cell growth by arresting their proliferation within definite, well-known checkpoints [75,76]. After cancerous cells were treated with anti-tumour agents, distinguishing cells in different cell cycle phases could be detected. MCF-7 cells have been treated with 1-benzyl-5-bromo-3-hydrazoneindolin-2-one **7d** at the IC<sub>50</sub>. Analyzing the gathered data reveals that compound **7d** significantly increased the number of cells in the sub-G1 phase compared to the control (9.7% vs. 0.8). It also resulted in a cell cycle arrest at the G2/M phase when compared to untreated cells (15.5% vs. 9.3%; Figure 2).

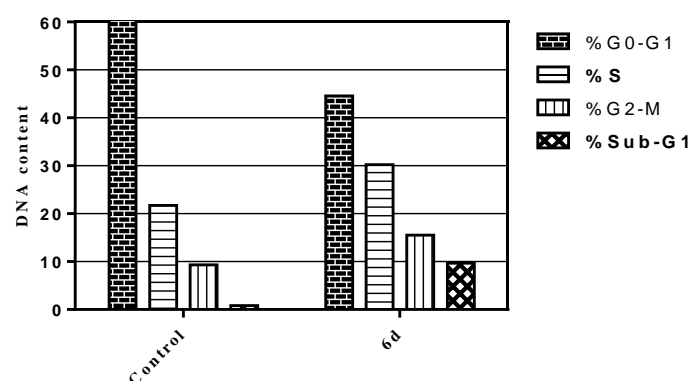


**Figure 2.** Effect of **7d** on the cell cycle phases within MCF-7 cells after treatment for 24 h at the IC<sub>50</sub> concentration.

### 2.3. Molecular Modeling

#### 2.3.1. Docking Studies

In structural molecular biology and computer-assisted drug design, molecular docking is an essential technique. The objective of ligand–protein docking is to determine the most probable binding mode(s) between a ligand and a protein whose three-dimensional structure is known [77]. In this study, the 4ASD PDB file was used to perform the docking study of our newly synthesised molecule **7d** on the VEGFR2 active site. The reference drug Sorafenib was used as a guide to identifying the active binding site with the important key amino acid residues.

Sorafenib shows a binding energy score of  $-16.4$  kcal/mol and forms hydrogen bonding interactions with Glu885, Cys919, and Asp1046 amino acid residues through its nitrogen atoms and carbonyl oxygen (Figure 3). Compound **7d** showed a comparable good binding score of  $-15.6$  kcal/mol. It also has a similar binding pattern, as it binds to Glu885 through hydrogen bonding with N, Asp106 through arene-H interaction, and Cys919 through halogen bonding with chlorine. These essential binding forces were supported by more interactions with Lys868, Val899 (hydrogen bonding), and several hydrophobic bindings with the aryl moieties (Figure 4).

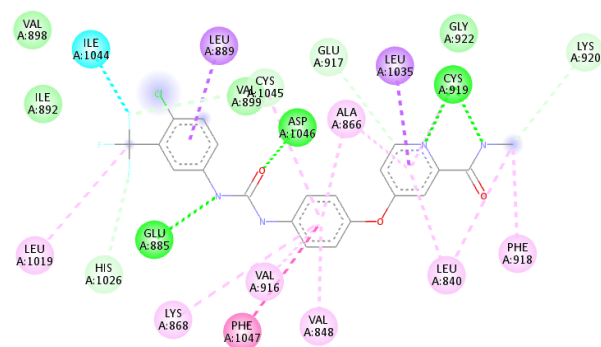


**Figure 3.** 2D interaction of sorafenib with the VEGFR2 active binding site.

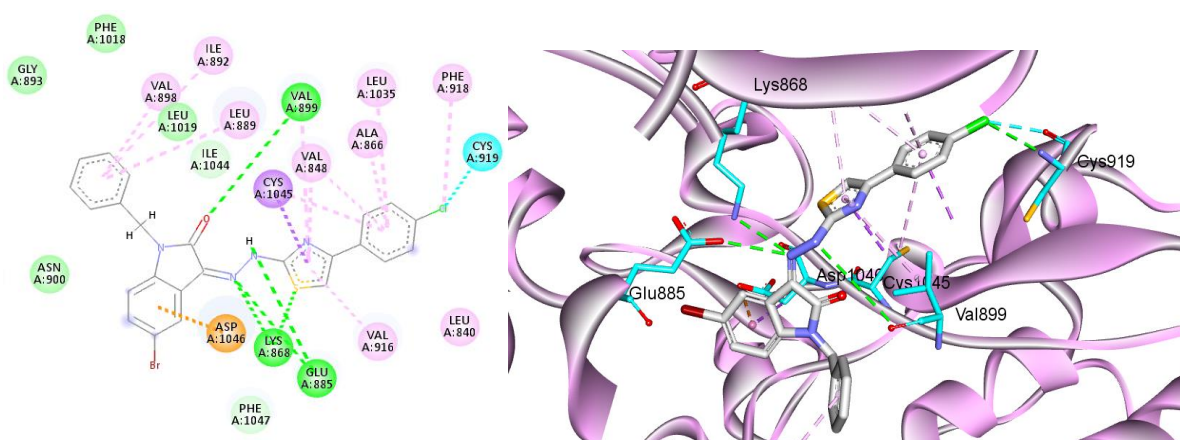


**Figure 4.** 2D and 3D interactions of compound **7d** with the VEGFR2 active binding site.

### 2.3.2. Molecular Dynamics

In several computational and molecular modelling investigations, molecular dynamics (MD) offers numerous crucial parameters, data, and figures. The exact assessment of the strength of the binding between a ligand and its target is one of the MD's most often used applications. The composition of macromolecules and characterizing the impact of certain mutations on the resistance profile of various medications are two more well-reported uses [78]. As a result, it made logistical sense to use the MD's advantages to support the biological and docking results for compound **7d**. Two MD simulation experiments were applied to compound **7d** bound to VEGFR-2 in addition to the x-ray coordinates of Sorafenib bound to VEGFR-2. It is interesting to note that the computed RMSD for compound **7d** reached 1.9 Å, while the RMSD of the Sorafenib complex reached 1.85 Å at their average deviations (Figure 5). The fact that compound **7d** can produce similar RMSD values to those of Sorafenib is a strong sign of its ability to form a stable complex with VEGFR-2.

As expected, the acquired findings from the RMSF computations for each of the two complexes' residues were very similar to the RMSD values. In comparison to the co-crystallized Sorafenib-VEGFR-2 complex, the compound **7d**-VEGFR-2 complex had a similar result in the residues fluctuation (Figure 6). The residue of VEGFR-2 after the binding of compound **7d** had average RMSF values of 1.52 Å while sorafenib induced average RMSF values of 1.47 Å. Given the ability of compound **7d** to produce similar values of RMSD and RMSF to Sorafenib, it is projected that VEGFR-2 is the main target for compound **7d**.

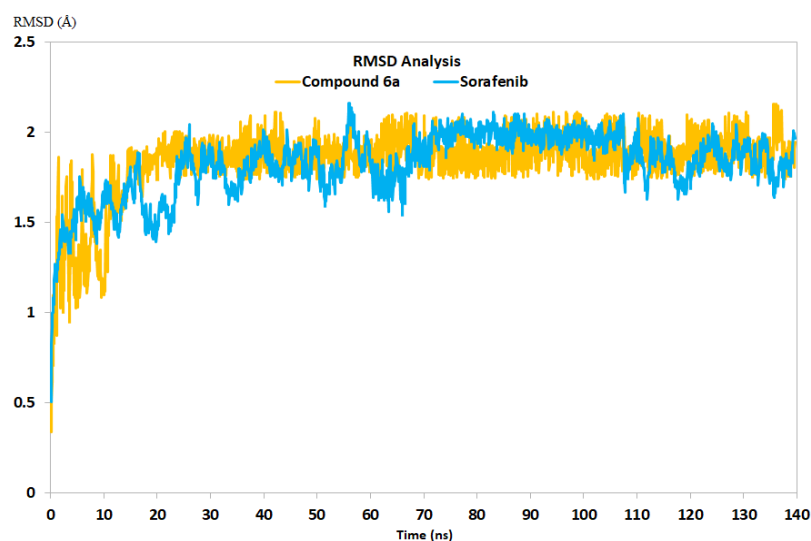


Figure 5. The RMSD values for sorafenib-VEGFR-2 (blue) and compound 7d-VEGFR-2 (orange).

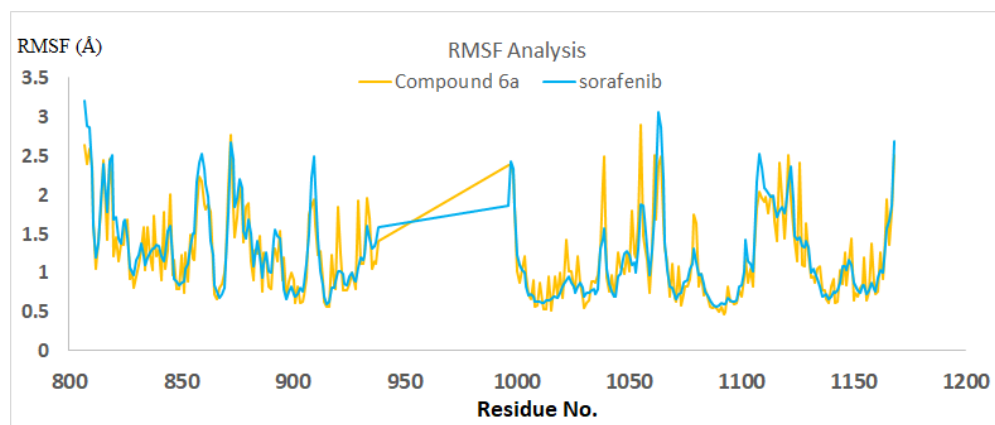


Figure 6. The RMSD values for sorafenib- VEGFR-2 (blue) and compound 7d-VEGFR-2 (orange).

### 3. Conclusions

With the prime aim of developing novel anti-tumour agents, this study reported the design and synthesis of two small molecule series (7a–d and 12a–e) based on the 1-benzyl-5-bromoindolin-2-one scaffold that connected through a hydrazone linker to a 4-arylthiazole (7a–d) or 4-methyl-5-(aryldiazenyl)thiazole (12a–e) moiety. The target molecules displayed cell growth inhibitory activities toward breast (MCF-7) and lung (A-549) cancer cell lines in variable degrees. In particular, the 4-arylthiazole bearing derivatives 7c and 7d revealed the best anticancer activity toward MCF-7 cells ( $IC_{50} = 7.17 \pm 0.94$  and  $2.93 \pm 0.47$ , respectively). Furthermore, both molecules disclosed good VEGFR-2 inhibitory activity, and their  $IC_{50}$  values were equal to  $0.728 \mu\text{M}$  and  $0.503 \mu\text{M}$ , respectively. Additionally, the impacts of 7d on the cell cycle phases as well as on the levels of different apoptotic markers (caspase-3, caspase-9, Bax, and Bcl-2) were assessed. Collectively, the upregulation of Bax, the increase in the ratio of Bax to Bcl-2, and the downregulation of Bcl-2 all pointed to the suggestion that compound 7d has a pro-apoptotic effect. Finally, molecular modelling studies have been carried out to rationalise the VEGFR-2 inhibitory activity of target compounds. The docking analysis disclosed the ability of 7d to achieve the essential interactions within the VEGFR-2 active site. Moreover, MD analysis revealed the ability of compound 7d to produce similar values of RMSD and RMSF to Sorafenib.

## 4. Experimental

### 4.1. Chemistry

#### 4.1.1. General

The NMR spectra were recorded by a Bruker Avance III 400 MHz high-performance digital FT-NMR spectrophotometer.  $^1\text{H}$  and  $^{13}\text{C}$  spectra were run at 400 and 100 MHz, respectively, in deuterated dimethylsulphoxide ( $\text{DMSO-}d_6$ ). All coupling constant ( $J$ ) values are given in hertz. Chemical shifts ( $\delta_{\text{C}}$ ) are reported relative to  $\text{DMSO-}d_6$  as internal standards. IR spectra were recorded as potassium bromide discs on a Shimadzu FT-IR 8400S spectrophotometer.

*N*-Benzyl-5-bromoindoline-2,3-dione **3** [79], 2-bromo-1-arylethanones **6a–d** [80], and 2-oxo-*N'*-(4-substitutedphenyl) propanehydrazonoyl chloride **11a–e** [81] were prepared as reported earlier.

#### 4.1.2. 2-(1-Benzyl-5-bromo-2-oxoindolin-3-ylidene)hydrazine-1-carbothioamide **4**

To a hot stirred solution of *N*-benzyl-5-bromoindoline-2,3-dione **3** (2.5 g, 8.0 mmol) in ethanol (15 mL) and cat. HOAc, thiosemicarbazide (0.9 g, 10 mmol) was added. Stirring then continued at the refluxing temperature for 5 h. The precipitate was filtered, washed with cooled ethanol, dried, and recrystallized from glacial acetic acid to afford the key intermediate **4** (yield 40%), m.p. 241–243 °C;  $^1\text{H}$  NMR ( $\text{DMSO-}d_6$ )  $\delta$  ppm: 4.956 (s, 2 H, benzylic protons), 6.94 (d, 1 H, Ar-H,  $J = 8.4$  Hz), 7.25–7.35 (m, 5 H, Ar-H), 7.48 (dd, 1 H, Ar-H,  $J = 8.4, 2.0$  Hz), 7.92 (d, 1 H, Ar-H,  $J = 2.0$  Hz), 8.86 (s, 1 H, NH), 9.15 (s, 1 H, NH), 12.21 (s, 1 H, NH);  $^{13}\text{C}$  NMR ( $\text{DMSO-}d_6$ )  $\delta$  ppm: 43.04, 112.73, 115.43, 122.27, 123.79, 127.82, 127.88, 128.09, 129.15, 129.99, 133.41, 135.89, 142.00, 160.89, 179.23; Anal. Calcd. for  $\text{C}_{16}\text{H}_{13}\text{BrN}_4\text{OS}$ : C, 49.37; H, 3.37; N, 14.39, found C, 49.22; H, 3.39; N, 14.43 [82,83].

#### 4.1.3. General Procedure for the Preparation of 1-benzyl-5-bromo-3-(2-(4-arylthiazol-2-yl)hydrazono)indolin-2-one **7a–d**

The key intermediate **4** (0.2 g, 0.5 mmol) was added to a solution of the appropriate 2-bromo-1-arylethanone **6a–d** (0.55 mmol) in ethanol (8 mL). The mixture was refluxed for seven hours. The precipitate was recovered by filtration while hot, washed with diethyl ether, dried, and recrystallized from methanol/DMF to provide the desired isatin derivatives **7a–d** with yields ranging from 69 to 81%.

#### 4.1.4. General Procedure for Preparation of 1-benzyl-5-bromo-3-(2-(4-methyl-5-(aryldiazenyl)thiazol-2-yl)hydrazono)indolin-2-ones **12a–e**

The key intermediate **4** (0.2 g, 0.5 mmol) was added to a solution of the appropriate hydrazonoyl chloride derivative **11a–e** (0.5 mmol) in dioxane (8 mL) in the presence of a catalytic amount of triethylamine. For 5 h, the reaction mixture was refluxed. The precipitate was recovered by filtering while hot, washed with ethanol, dried, and recrystallized from ethanol/DMF to obtain isatin derivatives **12a–e** with a yield of 58–70%.

### 4.2. Pharmacological Assays

The experimental procedures for the performed pharmacological assays. MTT cytotoxicity [84–86], VEGFR-2 inhibitory activity [87,88], and cell cycle flow cytometry [89] assays, as well as the assessment of the expression levels for the apoptotic markers [89], were described in the Supplementary Materials and performed as previously described.

### 4.3. Molecular Modeling Studies

#### 4.3.1. Docking Studies

The entire docking investigation was carried out using Vina Autodock software [90]. The VEGFR-2 crystal structure was acquired from the protein data bank using the PDB IDs: 4ASD. Chemdraw was used to draw a hybrid **7d**, which was then transformed into a 3D structure using the Biovia Discovery Visualizer. Because Vina Autodock re-

quires the receptor and ligands to be in pdbqt format, MGL tools were developed to produce the necessary pdbqt files. Furthermore, the active site was built by constructing a grid box around the binding of the co-crystallised sorafenib with dimensions of 20, 20, and 20 in the X, Y, and Z axes, respectively. Finally, hybrid **7d** was docked onto the VEGFR-2 predetermined active site. The docking findings were displayed using the free Biovia Discovery Studio 2021 visualizer, which generated 2D and 3D interactions for the docked poses.

#### 4.3.2. Molecular Dynamics

Groningen Machine for Chemical Simulations (GROMACS) 5.1.1 software was used to run the necessary molecular dynamics (MD) simulations [91]. Two molecular dynamic simulations (MDS) were performed using the 3D coordinates of VEGFR-2 in a complex with sorafenib and hybrid **7d**. The topologies of hybrid **7d** and sorafenib were generated using the GlycoBioChem PRODRG2 Server under the GROMOS96 force field [92]. The protein topology was generated using the pdb2gmx function embedded in the GROMACS software and then joined with each ligand topology to produce two o protein-ligand complexes. A typical workflow of GROMACS simulations was applied to the two complexes, starting with solvation using the recommended single point charge (SPC) water model, followed by adding the suitable number of counter-ions to neutralise the two complexes [93–96]. Energy-minimised complexes were obtained by applying a maximum of 50,000 steps of steepest descent minimization under the GROMOS96 53A6 force field using a Cutoff less than 10.0 kJ/mol. As a core step, the two complexes were equilibrated to the desired temperature (310 K) and pressure (1 atm) using both NVT and NPT ensembles for 8 ns and 2 ns, respectively. The particle mesh Ewald (PME) technique with a 12 cut-off and 12 Fourier spacing was used to calculate the long-range electrostatic values. All the systems underwent a 150 ns production stage. The structural coordinates were stored every 30 ps, and every two subsequent steps were separated by 2 fs. Throughout the simulation, the temperature (310 K) and the pressure (1 atm) were controlled via the Parrinello-Rahman technique and the V-rescale weak coupling method (a modified Berendsen thermostat) [97,98]. The obtained trajectories from the production stage were used to determine the root means square deviation (RMSD) and root mean square fluctuation (RMSF) of the overall system and each residue, respectively.

**Supplementary Materials:** The following supporting information can be downloaded at: <https://www.mdpi.com/article/10.3390/molecules28073203/s1>, Spectra and Elemental data for target compounds.

**Author Contributions:** Conceptualization, Z.M.E., N.A., R.R.A. and W.M.E.; Methodology, T.A.-W., H.A., Z.M.E., O.J.A., H.A.G. and M.K.E.-A.; Software, R.M.M., M.A.E.H., N.A. and H.A.G.; Validation, H.A., Z.M.E., M.A.E.H., R.R.A., W.M.E. and M.K.E.-A.; Formal analysis, T.A.-W., R.M.M., O.J.A., N.A., W.M.E. and M.K.E.-A.; Investigation, M.A.E.H.; Resources, T.A.-W. and H.A.; Data curation, R.M.M. and O.J.A.; Writing—original draft, H.A., R.M.M., M.A.E.H., H.A.G., W.M.E. and M.K.E.-A.; Writing—review & editing, T.A.-W., R.M.M., R.R.A. and M.K.E.-A.; Supervision, R.R.A. and W.M.E.; Project administration, W.M.E.; Funding acquisition, T.A.-W. and O.J.A. All authors have read and agreed to the published version of the manuscript.

**Funding:** The authors extend their appreciation to the Deanship of Scientific Research at Princess Nourah bint Abdulrahman University for funding this research through the Research Groups Program Grant no. (RGP-1440-0025)(2).

**Institutional Review Board Statement:** Not applicable.

**Informed Consent Statement:** Not applicable.

**Data Availability Statement:** Not applicable.

**Acknowledgments:** This research was funded by the Deanship of Scientific Research at Princess Nourah bint Abdulrahman University through the Research Groups Program Grant no. (RGP-1440-0025)(2).

**Conflicts of Interest:** The authors declare no conflict of interest.

**Sample Availability:** Samples of the compounds 6 and 8 are available from the authors.

## References

1. Siegel, R.L.; Kimberly, D.M.; Hannah, E.F.; Jemal, A. Cancer statistics, 2022. *CA A Cancer J. Clin.* **2022**, *72*, 7–33. [[CrossRef](#)]
2. Barreca, M.; Spanò, V.; Rocca, R.; Bivacqua, R.; Abel, A.-C.; Maruca, A.; Montalbano, A.; Raimondi, M.V.; Tarantelli, C.; Gaudio, E.; et al. Development of [1, 2] oxazoloisoindoles tubulin polymerization inhibitors: Further chemical modifications and potential therapeutic effects against lymphomas. *Eur. J. Med. Chem.* **2022**, *243*, 114744. [[CrossRef](#)] [[PubMed](#)]
3. Liu, J.; Zhu, X.; Yu, L.; Mao, M. Discovery of novel sulphonamide hybrids that inhibit LSD1 against bladder cancer cells. *J. Enzym. Inhib. Med. Chem.* **2022**, *37*, 866–875. [[CrossRef](#)]
4. Labbozzetta, M.; Barreca, M.; Spanò, V.; Raimondi, M.V.; Poma, P.; Notarbartolo, M.; Barraja, P.; Alessandra, M. Novel insights on [1, 2] oxazolo [5, 4-e] isoindoles on multidrug resistant acute myeloid leukemia cell line. *Drug. Dev. Res.* **2022**, *83*, 1331–1341. [[CrossRef](#)]
5. Sabt, A.; Eldehna, W.M.; Al-Warhi, T.; Alotaibi, O.J.; Elaasser, M.M.; Suliman, H.; Abdel-Aziz, H.A. Discovery of 3,6-disubstituted pyridazines as a novel class of anticancer agents targeting cyclin-dependent kinase 2: Synthesis, biological evaluation and in silico insights. *J. Enzym. Inhib. Med. Chem.* **2020**, *35*, 1616–1630. [[CrossRef](#)] [[PubMed](#)]
6. Al-Warhi, T.; Al-Karmalawy, A.A.; Elmaaty, A.A.; Alshubramy, M.A.; Abdel-Motaal, M.; Majrashi, T.A.; Asem, M.; Nabil, A.; Eldehna, W.M.; Sharaky, M. Biological evaluation, docking studies, and in silico ADME prediction of some pyrimidine and pyridine derivatives as potential EGFRWT and EGFR790M inhibitors. *J. Enzym. Inhib. Med. Chem.* **2023**, *38*, 176–191. [[CrossRef](#)] [[PubMed](#)]
7. Al-Ghulikah, H.A.; El-Sebaey, S.A.; Bass, A.K.A.; El-Zoghbi, M.S. New Pyrimidine-5-Carbonitriles as COX-2 Inhibitors: Design, Synthesis, Anticancer Screening, Molecular Docking, and In Silico ADME Profile Studies. *Molecules* **2022**, *27*, 7485. [[CrossRef](#)]
8. Chao, M.-W.; Lin, T.E.; HuangFu, W.-C.; Chang, C.-D.; Tu, H.-J.; Chen, L.-C.; Yen, S.-C.; Sung, T.-Y.; Huang, W.-J.; Yang, C.-R.; et al. Identification of a dual TAOK1 and MAP4K5 inhibitor using a structure-based virtual screening approach. *J. Enzym. Inhib. Med. Chem.* **2020**, *36*, 98–108. [[CrossRef](#)]
9. Alanazi, M.M.; Elwan, A.; Alsaif, N.A.; Obaidullah, A.J.; Alkahtani, H.M.; Al-Mehizia, A.A.; Alsubaie, S.M.; Taghour, M.S.; Ibrahim, H.E. Discovery of new 3-methylquinoxalines as potential anti-cancer agents and apoptosis inducers targeting VEGFR-2: Design, synthesis, and in silico studies. *J. Enzym. Inhib. Med. Chem.* **2021**, *36*, 1732–1750. [[CrossRef](#)]
10. Pralhad, T.; Madhusudan, S.; Rajendrakumar, K. Concept, mechanisms and therapeutics of angiogenesis in cancer and other diseases. *J. Pharm. Pharmacol.* **2003**, *55*, 1045–1053. [[CrossRef](#)]
11. Shibuya, M. Vascular endothelial growth factor (VEGF) and its receptor (VEGFR) signaling in angiogenesis: A crucial target for anti- and pro-angiogenic therapies. *Genes. Cancer* **2011**, *2*, 1097–1105. [[CrossRef](#)]
12. Abhinand, C.S.; Raju, R.; Soumya, S.J.; Arya, P.S.; Sudhakaran, P.R. VEGF-A/VEGFR2 signaling network in endothelial cells relevant to angiogenesis. *J. Cell. Commun. Signal.* **2016**, *10*, 347–354. [[CrossRef](#)] [[PubMed](#)]
13. Cheke, R.S.; Patil, V.M.; Firke, S.D.; Ambhore, J.P.; Ansari, I.A.; Patel, H.M.; Shinde, S.D.; Pasupuleti, V.R.; Hassan, I.; Adnan, M.; et al. Therapeutic outcomes of isatin and its derivatives against multiple diseases: Recent developments in drug discovery. *Pharmaceuticals* **2022**, *15*, 272. [[CrossRef](#)] [[PubMed](#)]
14. Guo, H. Isatin derivatives and their anti-bacterial activities. *Eur. J. Med. Chem.* **2018**, *164*, 678–688. [[CrossRef](#)] [[PubMed](#)]
15. De Moraes Gomes, P.A.T.; Pena, L.J.; Leite, A.C.L. Isatin derivatives and their antiviral properties against arboviruses: A review. *Mini Rev. Med. Chem.* **2019**, *19*, 56–62. [[CrossRef](#)]
16. Eldehna, W.M.; Fares, M.; Ibrahim, H.S.; Alsherbiny, M.A.; Aly, M.H.; Ghabbour, H.A.; Abdel-Aziz, H.A. Synthesis and cytotoxic activity of biphenylurea derivatives containing indolin-2-one moieties. *Molecules* **2016**, *16*, 762. [[CrossRef](#)] [[PubMed](#)]
17. Kumar, H.M.S.; Herrmann, L.; Tsogoeva, S.B. Structural hybridization as a facile approach to new drug candidates. *Bioorganic Med. Chem. Lett.* **2020**, *30*, 127514. [[CrossRef](#)]
18. Ding, Z.; Zhou, M.; Zeng, C. Recent advances in isatin hybrids as potential anticancer agents. *Arch. Der. Pharm.* **2020**, *353*, e1900367. [[CrossRef](#)]
19. Hou, Y.; Shang, C.; Wang, H.; Jie, Y. Isatin-azole hybrids and their anticancer activities. *Arch. Der. Pharm.* **2020**, *353*, 1900272. [[CrossRef](#)]
20. De Paiva, R.E.F.; Vieira, E.G.; da Silva, D.R.; Wegermann, C.A.; Ferreira, A.M.C. Anticancer compounds based on isatin-derivatives: Strategies to ameliorate selectivity and efficiency. *Front. Mol. Biosci.* **2021**, *7*, 627272. [[CrossRef](#)]
21. Eldehna, W.M.; Altoukhy, A.; Mahrous, H.; Abdel-Aziz, H.A. Design, synthesis and QSAR study of certain isatin-pyridine hybrids as potential anti-proliferative agents. *Eur. J. Med. Chem.* **2015**, *90*, 684–694. [[CrossRef](#)] [[PubMed](#)]
22. Eldehna, W.M.; Al-Wabli, R.I.; Almutairi, M.S.; Keeton, A.B.; Piazza, G.A.; Abdel-Aziz, H.; Attia, M.I. Synthesis and biological evaluation of certain hydrazonoindolin-2-one derivatives as new potent anti-proliferative agents. *J. Enzym. Inhib. Med. Chem.* **2018**, *33*, 867–878. [[CrossRef](#)] [[PubMed](#)]
23. Zhang, L.; Xu, Z. Coumarin-containing hybrids and their anticancer activities. *Eur. J. Med. Chem.* **2019**, *181*, 111587. [[CrossRef](#)]
24. Eldehna, W.M.; El Hassab, M.A.; Abo-Ashour, M.F.; Al-Warhi, T.; Elaasser, M.M.; Safwat, N.A.; Suliman, H.; Ahmed, M.F.; Al-Rashood, S.T.; Abdel-Aziz, H.A.; et al. Development of isatin-thiazolo [3, 2-a] benzimidazole hybrids as novel CDK2 inhibitors

- with potent in vitro apoptotic anti-proliferative activity: Synthesis, biological and molecular dynamics investigations. *Bioorganic Chem.* **2021**, *110*, 104748. [[CrossRef](#)] [[PubMed](#)]
25. Eldehna, W.M.; Salem, R.; Elsayed, Z.M.; Al-Warhi, T.; Knany, H.R.; Ayyad, R.R.; Traiki, B.T.; Abdulla, M.-H.; Ahmad, R.; Abdel-Aziz, H.A.; et al. Development of novel benzofuran-isatin conjugates as potential antiproliferative agents with apoptosis inducing mechanism in Colon cancer. *J. Enzym. Inhib. Med. Chem.* **2021**, *36*, 1423–1434. [[CrossRef](#)]
  26. Eldehna, W.M.; Al-Rashood, S.T.; Al-Warhi, T.; Eskandrani, R.O.; Alharbi, A.; Ahmed, M.E.K. Novel oxindole/benzofuran hybrids as potential dual CDK2/GSK-3 $\beta$  inhibitors targeting breast cancer: Design, synthesis, biological evaluation, and in silico studies. *J. Enzym. Inhib. Med. Chem.* **2021**, *36*, 271–286. [[CrossRef](#)]
  27. Eldehna, W.M.; Almahli, H.; Al-Ansary, G.H.; Ghabbour, H.A.; Aly, M.H.; Ismael, O.E.; Al-Dhfyhan, A.; Abdel-Aziz, H.A. Synthesis and in vitro anti-proliferative activity of some novel isatins conjugated with quinazoline/phthalazine hydrazines against triple-negative breast cancer MDA-MB-231 cells as apoptosis-inducing agents. *J. Enzym. Inhib. Med. Chem.* **2017**, *32*, 600–613. [[CrossRef](#)]
  28. Abdel-Aziz, H.A.; Eldehna, W.M.; Keeton, A.B.; Piazza, G.A.; Kadi, A.A.; Attwa, M.W.; Abdelhameed, A.S.; Attia, M.I. Isatin-benzoxazine molecular hybrids as potential antiproliferative agents: Synthesis and in vitro pharmacological profiling. *Drug Des. Dev. Ther.* **2017**, *11*, 2333–2346. [[CrossRef](#)]
  29. Al-Warhi, T.; Abo-Ashour, M.F.; Almahli, H.; Alotaibi, O.J.; Al-Sanea, M.M.; Al-Ansary, G.H.; Ahmed, H.Y.; Elaasser, M.M.; Eldehna, W.M.; Abdel-Aziz, H.A. Novel [(N-alkyl-3-indolylmethylene) hydrazono] oxindoles arrest cell cycle and induce cell apoptosis by inhibiting CDK2 and Bcl-2: Synthesis, biological evaluation and in silico studies. *J. Enzym. Inhib. Med. Chem.* **2020**, *35*, 1300–1309. [[CrossRef](#)]
  30. Al-Warhi, T.; El Kerdawy, A.M.; Aljaeed, N.; Ismael, O.E.; Ayyad, R.R.; Eldehna, W.M.; Abdel-Aziz, H.A.; Al-Ansary, G.H. Synthesis, biological evaluation and in silico studies of certain oxindole–indole conjugates as anticancer CDK inhibitors. *Molecules* **2020**, *25*, 2031. [[CrossRef](#)]
  31. El-Naggar, M.; Eldehna, W.M.; Almahli, H.; Elgez, A.; Fares, M.; Elaasser, M.M.; Abdel-Aziz, H.A. Novel thiazolidinone/thiazolo [3, 2-a] benzimidazolone-isatinas apoptotic anti-proliferative agents towards breast cancer: One-pot synthesis and in vitro biological evaluation. *Molecules* **2018**, *23*, 1420. [[CrossRef](#)]
  32. Boda, S.; Nukala, S.K.; Ravinder, M. One-Pot Synthesis of Some New Isatin-1,2,4-oxadiazole Hybrids as VEGFR-2 Aiming Anticancer Agents. *ChemistrySelect* **2022**, *7*, e202200972. [[CrossRef](#)]
  33. Dhokne, P.; Sakla, A.P.; Shankaraiah, N. Structural insights of oxindole based kinase inhibitors as anticancer agents: Recent advances. *Eur. J. Med. Chem.* **2021**, *216*, 113334. [[CrossRef](#)]
  34. Seliem, I.A.; Panda, S.S.; Girgis, A.S.; Tran, Q.L.; Said, M.F.; Bekheit, M.S.; Abdelnaser, A.; Nasr, S.; Fayad, W.; Soliman, A.A.; et al. Development of Isatin-Based Schiff Bases Targeting VEGFR-2 Inhibition: Synthesis, Characterization, Antiproliferative Properties, and QSAR Studies. *ChemMedChem* **2022**, *17*, e202200164. [[CrossRef](#)] [[PubMed](#)]
  35. Srour, A.M.; Dawood, D.H.; Nossier, E.S.; El-Shiekh, R.A.; Mahmoud, A.E.; Hussien, A.G.; Omran, M.M.; Ali, M.M. Design, synthesis and molecular docking simulation of oxindole-based derivatives with dual VEGFR-2 and cholinesterase inhibitory activities. *J. Mol. Struct.* **2023**, *1271*, 134130. [[CrossRef](#)]
  36. Pathak, A.; Pandey, V.; Pokharel, Y.R.; Devaraji, V.; Ali, A.; Haider, K.; Saad, S.; Dewangan, R.P.; Siddiqui, N.; Yar, M.S. Pharmacophore based drug design and synthesis of oxindole bearing hybrid as anticancer agents. *Bioorganic Chem.* **2021**, *116*, 105358. [[CrossRef](#)]
  37. Zou, Y. Benzofuran-isatin conjugates as potent VEGFR-2 and cancer cell growth inhibitors. *J. Heterocycl. Chem.* **2020**, *57*, 510–516. [[CrossRef](#)]
  38. Abdelgawad, M.A.; Hayallah, A.M.; Bukhari, S.N.A.; Musa, A.; Elmowafy, M.; Abdel-Rahman, H.M.; El-Gaber, A.; Mohammed, K. Design, Synthesis, Molecular Modeling, and Anticancer Evaluation of New VEGFR-2 Inhibitors Based on the Indolin-2-One Scaffold. *Pharmaceuticals* **2022**, *15*, 1416. [[CrossRef](#)]
  39. Yang, T.-H.; Lee, C.-I.; Huang, W.-H.; Lee, A.-R. Synthesis and evaluation of novel 2-pyrrolidone-fused (2-oxoindolin-3-ylidene) methylpyrrole derivatives as potential multi-target tyrosine kinase receptor inhibitors. *Molecules* **2017**, *22*, 913. [[CrossRef](#)]
  40. Al-Salem, H.S.; Arifuzzaman, M.; Issa, I.S.; Motiur Rahman, A.F.M. Isatin-hydrazones with multiple Receptor Tyrosine Kinases (RTKs) inhibitory activity and in-silico binding mechanism. *Appl. Sci.* **2021**, *11*, 3746. [[CrossRef](#)]
  41. Chang, Y.; Yuan, Y.; Zhang, Q.; Rong, Y.; Yang, Y.; Chi, M.; Liu, Z.; Zhang, Y.; Yu, P.; Teng, Y. Effects of an isatin derivative on tumor cell migration and angiogenesis. *RSC Adv.* **2020**, *10*, 1191–1197. [[CrossRef](#)]
  42. Kang, C.-M.; Liu, D.-Q.; Zhao, X.-H.; Dai, Y.-J.; Cheng, J.-G.; Lv, Y.-T. QSAR and molecular docking studies on oxindole derivatives as VEGFR-2 tyrosine kinase inhibitors. *J. Recept. Signal. Transduct.* **2015**, *36*, 1–7. [[CrossRef](#)] [[PubMed](#)]
  43. Yang, T.-H.; Lee, C.-I.; Huang, W.-H.; An-Rong, L. Structural optimization and evaluation of novel 2-pyrrolidone-fused (2-oxoindolin-3-ylidene) methylpyrrole derivatives as potential VEGFR-2/PDGFR $\beta$  inhibitors. *Chem. Cent. J.* **2017**, *11*, 1–17. [[CrossRef](#)] [[PubMed](#)]
  44. Wang, D.-P.; Liu, K.-L.; Li, X.-Y.; Lu, G.-Q.; Xue, W.-H.; Qian, X.-H.; Meng, F.-H. Design, synthesis, and in vitro and in vivo anti-angiogenesis study of a novel vascular endothelial growth factor receptor-2 (VEGFR-2) inhibitor based on 1,2,3-triazole scaffold. *Eur. J. Med. Chem.* **2020**, *211*, 113083. [[CrossRef](#)] [[PubMed](#)]



45. Eldehna, W.M.; Fares, M.; Ibrahim, H.S.; Aly, M.H.; Zada, S.; Ali, M.M.; Abou-Seri, S.M.; Abdel-Aziz, H.A.; Abou El Ella, D.A. Indoline ureas as potential anti-hepatocellular carcinoma agents targeting VEGFR-2: Synthesis, in vitro biological evaluation and molecular docking. *Eur. J. Med. Chem.* **2015**, *100*, 89–97. [[CrossRef](#)]
46. Mohamady, S.; Galal, M.; Eldehna, W.M.; Gutierrez, D.C.; Ibrahim, H.S.; Elmazar, M.M.; Ali, H.I. Dual Targeting of VEGFR2 and C-Met Kinases via the Design and Synthesis of Substituted 3-(Triazolo-thiadiazin-3-yl) indolin-2-one Derivatives as Angiogenesis Inhibitors. *ACS Omega* **2020**, *5*, 18872–18886. [[CrossRef](#)]
47. Elkaeed, E.B.; Taghour, M.S.; Mahdy, H.A.; Eldehna, W.M.; El-Deeb, N.M.; Kenawy, A.M.; Alsouk, B.A.; Dahab, M.A.; Metwaly, A.M.; Eissa, I.H.; et al. New quinoline and isatin derivatives as apoptotic VEGFR-2 inhibitors: Design, synthesis, anti-proliferative activity, docking, ADMET, toxicity, and MD simulation studies. *J. Enzym. Inhib. Med. Chem.* **2022**, *37*, 2191–2205. [[CrossRef](#)]
48. Taghour, M.S.; Elkady, H.; Eldehna, W.M.; El-Deeb, N.M.; Kenawy, A.M.; Elkaeed, E.B.; Alsouk, A.A.; Alesawy, M.S.; Metwaly, A.M.; Ibrahim, H.E. Design and synthesis of thiazolidine-2, 4-diones hybrids with 1,2-dihydroquinolones and 2-oxindoles as potential VEGFR-2 inhibitors: In-vitro anticancer evaluation and in-silico studies. *J. Enzym. Inhib. Med. Chem.* **2022**, *37*, 1903–1917. [[CrossRef](#)]
49. Taghour, M.S.; Elkady, H.; Eldehna, W.M.; El-Deeb, N.; Kenawy, A.M.; Elkaeed, E.B.; Alsouk, B.A.; Alesawy, M.S.; Husein, D.Z.; Metwaly, A.M.; et al. Design, synthesis, anti-proliferative evaluation, docking, and MD simulations studies of new thiazolidine-2, 4-diones targeting VEGFR-2 and apoptosis pathway. *PLoS ONE* **2022**, *17*, e0272362. [[CrossRef](#)]
50. Abdelsalam, E.A.; El-Hafeez, A.A.A.; Eldehna, W.M.; El Hassab, M.A.; Marzouk, H.M.M.; Elaasser, M.M.; Taleb, N.A.A.; Amin, K.M.; Abdel-Aziz, H.A.; Ghosh, P.; et al. Discovery of novel thiazolyl-pyrazolines as dual EGFR and VEGFR-2 inhibitors endowed with in vitro antitumor activity towards non-small lung cancer. *J. Enzym. Inhib. Med. Chem.* **2022**, *37*, 2265–2282. [[CrossRef](#)]
51. King, L.C.; Ostrum, G.K. Selective Bromination with Copper(II) Bromide 1. *J. Org. Chem.* **1964**, *29*, 3459–3461. [[CrossRef](#)]
52. Al-Sanea, M.M.; Al-Ansary, G.H.; Elsayed, Z.M.; Maklad, R.M.; Elkaeed, E.B.; Abdelgawad, M.A.; Bukhari, S.N.A.; Abdel-Aziz, M.M.; Suliman, H.; Eldehna, W.M. Development of 3-methyl/3-(morpholinomethyl)benzofuran derivatives as novel antitumor agents towards non-small cell lung cancer cells. *J. Enzym. Inhib. Med. Chem.* **2021**, *36*, 987–999. [[CrossRef](#)] [[PubMed](#)]
53. Eldehna, W.M.; Maklad, R.M.; Almahli, H.; Al-Warhi, T.; Elkaeed, E.B.; Abourehab, M.A.S.; Abdel-Aziz, H.A.; El Kerdawy, A.M. Identification of 3-(piperazinylmethyl) benzofuran derivatives as novel type II CDK2 inhibitors: Design, synthesis, biological evaluation, and in silico insights. *J. Enzym. Inhib. Med. Chem.* **2022**, *37*, 1227–1240. [[CrossRef](#)] [[PubMed](#)]
54. Maklad, R.M.; AbdelHafez, E.-S.M.; Abdelhamid, D.; Aly, O.M. Tubulin inhibitors: Discovery of a new scaffold targeting extra-binding residues within the colchicine site through anchoring substituents properly adapted to their pocket by a semi-flexible linker. *Bioorganic. Chem.* **2020**, *99*, 103767. [[CrossRef](#)]
55. Ismail, R.S.; Abou-Seri, S.M.; Eldehna, W.M.; Ismail, N.S.; Elgazwi, S.M.; Ghabbour, H.A.; Ahmed, M.S.; Halaweish, F.T.; El Ella, D.A.A. Novel series of 6-(2-substitutedacetamido)-4-anilinoquinazolines as EGFR-ERK signal transduction inhibitors in MCF-7 breast cancer cells. *Eur. J. Med. Chem.* **2018**, *155*, 782–796. [[CrossRef](#)] [[PubMed](#)]
56. Ho, T.-L. Hard soft acids bases (HSAB) principle and organic chemistry. *Chem. Rev.* **1975**, *75*, 1–20. [[CrossRef](#)]
57. Aly, O.M.; Beshr, E.A.; Maklad, R.M.; Mustafa, M.; Gamal-Eldeen, A.M. Synthesis, Cytotoxicity, Docking Study, and Tubulin Polymerization Inhibitory Activity of Novel 1-(3,4-Dimethoxyphenyl)-5-(3,4,5-trimethoxyphenyl)-1H-1,2,4-triazole-3-carboxanilides: 1-(3,4-Dimethoxyphenyl)-5-(3,4,5-trimethoxyphenyl)-1H-1,2,4-triazole-3-carboxanilides. *Arch. Der. Pharm.* **2014**, *347*, 658–667. [[CrossRef](#)]
58. Elasasy, M.E.A.; Elnaggar, D.H.; Hafez, N.A.A.; Azab, M.E.; Amr, A.E.; Omran, M.M.; Mohamed, A.M. Synthesis and Antiproliferative Activity of Novel Hydrazono Thiazolidine and Thiazole Derivatives Bearing Rhodanine Moiety. *Russ. J. Gen. Chem.* **2021**, *91*, 915–925. [[CrossRef](#)]
59. Abdelhamid, A.O.; Sayed, A.R.; Zaki, Y.H. Reaction of Hydrazonoyl Halides 51<sup>1</sup>: A Facile Synthesis of 5-Arylthiazoles and Triazolino [4,3-*a*]pyrimidines as Antimicrobial Agents. *Phosphorus Sulfur Silicon Relat. Elements* **2007**, *182*, 1447–1457. [[CrossRef](#)]
60. Phillips, R.R. The Japp-Klingemann Reaction. In *Organic Reactions*; John Wiley & Sons, Inc., Ed.; John Wiley & Sons, Inc.: Hoboken, NJ, USA, 2011; pp. 143–178. [[CrossRef](#)]
61. Farghaly, M.; Abdel-Wahab, B.F.; Ahmed, E.M. Synthesis, antiviral and antimicrobial screening of some new 2-oxoindoline derivatives. *Chem. Heterocycl. Comp.* **2009**, *45*, 539–544. [[CrossRef](#)]
62. Sanad, S.M.H.; Mekky, A.E.M.; Said, A.Y.; Elneairy, M.A.A. Pyridine-2(1H)-thiones: Versatile precursors for one-pot synthesis of new Nicotinonitrile-Thiazole hybrids. *J. Heterocyclic. Chem.* **2021**, *58*, 1461–1471. [[CrossRef](#)]
63. Al-Hussain, S.A.; Alshehrei, F.; Zaki, M.E.A.; Harras, M.F.; Farghaly, T.A.; Muhammad, Z.A. Fluorinated hydrazonoyl chlorides as precursors for synthesis of antimicrobial azoles. *J. Heterocyclic. Chem.* **2020**, *58*, 589–602. [[CrossRef](#)]
64. Voronin, V.V.; Ledovskaya, M.S.; Gordeev, E.G.; Rodygin, K.S.; Ananikov, V.P. [3+2]-Cycloaddition of in Situ Generated Nitrile Imines and Acetylene for Assembling of 1,3-Disubstituted Pyrazoles with Quantitative Deuterium Labeling. *J. Org. Chem.* **2018**, *83*, 3819–3828. [[CrossRef](#)] [[PubMed](#)]
65. Sharma, P.; Bhat, S.V.; Prabhath, M.R.R.; Molino, A.; Nauha, E.; Wilson, D.J.D.; Moses, J.E. Synthesis of 4-Triazol-3-imines via Selective Stepwise Cycloaddition of Nitrile Imines with Organo-cyanamides. *Org. Lett.* **2018**, *20*, 4263–4266. [[CrossRef](#)]
66. Konkel, M.J.; Lagu, B.; Boteju, L.W.; Jimenez, H.; Noble, S.; Walker, M.W.; Chandrasena, G.; Blackburn, T.P.; Nikam, S.S.; Wright, J.L.; et al. 3-arylimino-2-indolones are potent and selective galanin GAL3 receptor antagonists. *J. Med. Chem.* **2006**, *49*, 3757–3758. [[CrossRef](#)] [[PubMed](#)]

67. Wegermann, C.A.; Monzani, E.; Casella, L.; Ribeiro, M.A.; Bruzeguini, C.E.; Vilcachagua, J.D.; Costa, L.A.S.; Ferreira, A.M.D.C. Unveiling geometrical isomers and tautomers of isatin-hydrazones by NMR spectroscopy. *J. Mol. Struct.* **2021**, *1250*, 131633. [[CrossRef](#)]
68. Jakusová, K.; Donovalová, J.; Gáplovský, M.; Cigáň, M.; Stankovičová, H.; Self-association, A.G. Self-association, tautomerism and E–Z isomerization of isatin–phenylsemicarbazones—spectral study and theoretical calculations. *J. Phys. Org. Chem.* **2013**, *26*, 805–813. [[CrossRef](#)]
69. Abdel-Aziz, H.A.; Ghabbour, H.A.; Eldehna, W.M.; Qabeel, M.M. Synthesis, crystal structure, and biological activity of cis/trans amide rotomers of (Z)-N'-(2-Oxoindolin-3-ylidene) formohydrazide. *J. Chem.* **2014**, *2014*, 760434. [[CrossRef](#)]
70. Sabt, A.; Eldehna, W.M.; Ibrahim, T.M.; Bekhit, A.A.; Rasha, Z.B. New antileishmanial quinoline linked isatin derivatives targeting DHFR-TS and PTR1: Design, synthesis, and molecular modeling studies. *Eur. J. Med. Chem.* **2023**, *246*, 114959. [[CrossRef](#)]
71. Pfeffer, C.M.; Singh, A.T. Apoptosis: A target for anticancer therapy. *Int. J. Mol. Sci.* **2018**, *19*, 448. [[CrossRef](#)]
72. Hu, W.; Kavanagh, J.J. Anticancer therapy targeting the apoptotic pathway. *Lancet Oncol.* **2003**, *4*, 721–729. [[CrossRef](#)] [[PubMed](#)]
73. Saleem, M.; Qadir, M.I.; Perveen, N.; Ahmad, B.; Saleem, U.; Irshad, T. Inhibitors of apoptotic proteins: New targets for anticancer therapy. *Chem. Biol. Drug. Des.* **2013**, *82*, 243–251. [[CrossRef](#)] [[PubMed](#)]
74. Reed, J.C. Apoptosis-based therapies. *Nat. Rev. Drug. Discov.* **2002**, *1*, 111–121. [[CrossRef](#)] [[PubMed](#)]
75. Bai, J.; Yaochen, L.; Guojun, Z. Cell cycle regulation and anticancer drug discovery. *Cancer Biol. Med.* **2017**, *14*, 348.
76. Eastman, A. Cell cycle checkpoints and their impact on anticancer therapeutic strategies. *J. Cell. Biochem.* **2004**, *91*, 223–231. [[CrossRef](#)]
77. Källblad, P.; Mancera, R.L.; Nikolay, P. Assessment of multiple binding modes in ligand–protein docking. *J. Med. Chem.* **2004**, *47*, 3334–3337. [[CrossRef](#)]
78. Tripathi, S.; Srivastava, G.; Ashok, S. Molecular dynamics simulation and free energy landscape methods in probing L215H, L217R and L225M  $\beta$ I-tubulin mutations causing paclitaxel resistance in cancer cells. *Biochem. Biophys. Res. Commun.* **2016**, *476*, 273–279. [[CrossRef](#)] [[PubMed](#)]
79. Karki, S.S.; Bahaduria, V.S.; Rana, V.; Kumar, S.; Subbaro, P.G.; Das, U.; Balzarini, J.; De Clercq, E.; Dimmock, J.R. 1-Arylmethyl-2, 3-dioxo-2, 3-dihydroindole thiosemicarbazones as leads for developing cytotoxins and anticonvulsants. *J. Enzym. Inhib. Med. Chem.* **2008**, *24*, 537–544. [[CrossRef](#)]
80. Da Costa, D.P.; de Castro, A.C.; da Silva, G.A.; Lima-Junior, C.G.; de Andrade Júnior, F.P.; de Oliveira Lima, E.; Vaz, B.G.; da Silva, L.C. Microwave-assisted synthesis and antimicrobial activity of novel spiro 1, 3, 4-thiadiazolines from isatin derivatives. *J. Heterocycl. Chem.* **2021**, *58*, 766–776. [[CrossRef](#)]
81. Eldehna, W.M.; Abo-Ashour, M.F.; Al-Warhi, T.; Al-Rashood, S.T.; Alharbi, A.; Ayyad, R.R.; Al-Khayal, K.; Abdulla, M.; Abdel-Aziz, H.A.; Ahmad, R.; et al. Development of 2-oxindolin-3-ylidene-indole-3-carbohydrazide derivatives as novel apoptotic and anti-proliferative agents towards colorectal cancer cells. *J. Enzym. Inhib. Med. Chem.* **2021**, *36*, 320–329. [[CrossRef](#)]
82. Abou-Seri, S.M.; Eldehna, W.M.; Ali, M.M.; El Ella, D.A.A. 1-Piperazinylphthalazines as potential VEGFR-2 inhibitors and anticancer agents: Synthesis and in vitro biological evaluation. *Eur. J. Med. Chem.* **2016**, *107*, 165–179. [[CrossRef](#)] [[PubMed](#)]
83. Abdel-Aziz, H.A.; Eldehna, W.M.; Fares, M.; Al-Rashood, S.T.A.; Al-Rashood, K.A.; Abdel-Aziz, M.M.; Soliman, D.H. Synthesis, biological evaluation and 2D-QSAR study of halophenyl bis-hydrazones as antimicrobial and antitubercular agents. *Int. J. Mol. Sci.* **2015**, *16*, 8719–8743. [[CrossRef](#)] [[PubMed](#)]
84. Mosmann, T. Rapid colorimetric assay for cellular growth and survival: Application to proliferation and cytotoxicity assays. *J. Immunol. Methods* **1983**, *65*, 55–63. [[CrossRef](#)]
85. Khalifa, M.M.; Al-Karmalawy, A.A.; Elkaeed, E.B.; Nafie, M.S.; Tantawy, M.A.; Eissa, I.H.; Mahdy, H.A. Topo II inhibition and DNA intercalation by new phthalazine-based derivatives as potent anticancer agents: Design, synthesis, anti-proliferative, docking, and in vivo studies. *J. Enzym. Inhib. Med. Chem.* **2021**, *37*, 299–314. [[CrossRef](#)]
86. Hagra, M.; El Deeb, M.A.; Elzahabi, H.S.A.; Elkaeed, E.B.; Mehany, A.B.M.; Eissa, I.H. Discovery of new quinolines as potent colchicine binding site inhibitors: Design, synthesis, docking studies, and anti-proliferative evaluation. *J. Enzym. Inhib. Med. Chem.* **2021**, *36*, 640–658. [[CrossRef](#)]
87. Nafie, M.S.; Boraie, A.T. Exploration of novel VEGFR2 tyrosine kinase inhibitors via design and synthesis of new alkylated indolyl-triazole Schiff bases for targeting breast cancer. *Bioorganic Chem.* **2022**, *122*, 105708. [[CrossRef](#)]
88. Rayes, E.; Samir, M.; El Enany, G.; Ali, I.A.I.; Ibrahim, W.; Mohamed, S.; Nafie, M.S. Synthesis of novel phthalazinedione-based derivatives with promising cytotoxic, anti-bacterial, and molecular docking studies as vegfr2 inhibitors. *ACS Omega* **2022**, *7*, 26800–26811. [[CrossRef](#)]
89. Eldehna, W.M.; Abo-Ashour, M.F.; Ibrahim, H.S.; Al-Ansary, G.H.; Ghabbour, H.A.; Elaasser, M.M.; Ahmed, H.Y.A.; Safwat, N.A. Novel [(3-indolylmethylene) hydrazono] indolin-2-ones as apoptotic anti-proliferative agents: Design, synthesis and in vitro biological evaluation. *J. Enzym. Inhib. Med. Chem.* **2018**, *33*, 686–700. [[CrossRef](#)]
90. Trott, O.; Olson, A.J. AutoDock Vina: Improving the speed and accuracy of docking with a new scoring function, efficient optimization, and multithreading. *J. Comput. Chem.* **2010**, *31*, 455–461. [[CrossRef](#)]
91. Abraham, M.J.; Murtola, T.; Schulz, R.; Páll, S.; Smith, J.C.; Hess, B.; Lindahl, E. GROMACS: High performance molecular simulations through multi-level parallelism from laptops to supercomputers. *SoftwareX* **2015**, *1*, 19–25. [[CrossRef](#)]
92. AW, S.; van Aalten, D.M.F. PRODRG: A tool for high-throughput crystallography of protein-ligand complexes. *Acta Cryst. D. Biol. Cryst.* **2004**, *60*, 1355–1363.

93. Hassab, M.A.E.; Fares, M.; Amin, M.K.A.H.; Al-Rashood, S.T.; Alharbi, A.; Eskandrani, R.O.; Alkahtani, H.M.; Eldehna, W.M. Toward the identification of potential  $\alpha$ -ketoamide covalent inhibitors for SARS-CoV-2 main protease: Fragment-based drug design and MM-PBSA calculations. *Processes* **2021**, *9*, 1004. [[CrossRef](#)]
94. El Hassab, M.A.; Shoun, A.A.; Al-Rashood, S.T.; Al-Warhi, T.; Eldehna, W.M. Identification of a new potential SARS-COV-2 RNA-dependent RNA polymerase inhibitor via combining fragment-based drug design, docking, molecular dynamics, and MM-PBSA calculations. *Front. Chem.* **2020**, *8*, 915. [[CrossRef](#)] [[PubMed](#)]
95. El Hassab, M.A.; Ibrahim, T.M.; Al-Rashood, S.T.; Alharbi, A.; Eskandrani, R.O.; Eldehna, W.M. In silico identification of novel SARS-COV-2 2'-O-methyltransferase (nsp16) inhibitors: Structure-based virtual screening, molecular dynamics simulation and MM-PBSA approaches. *J. Enzyme Inhib. Med. Chem.* **2021**, *36*, 727–736. [[CrossRef](#)] [[PubMed](#)]
96. El Hassab, M.A.; Ibrahim, T.M.; Shoun, A.A.; Al-Rashood, S.T.; Alkahtani, H.M.; Alharbi, A.; Eskandrani, R.O.; Eldehna, W.M. In silico identification of potential SARS COV-2 2'-O-methyltransferase inhibitor: Fragment-based screening approach and MM-PBSA calculations. *RSC Adv.* **2021**, *11*, 16026–16033. [[CrossRef](#)]
97. Berendsen, H.J.C.; Postma, J.P.M.; Van Gunsteren, W.F.; DiNola, A.; Haak, J.R. Molecular dynamics with coupling to an external bath. *J. Chem. Phys.* **1984**, *81*, 3684–3690. [[CrossRef](#)]
98. Parrinello, M.; Rahman, A. Polymorphic transitions in single crystals: A new molecular dynamics method. *J. Appl. Phys.* **1981**, *52*, 7182–7190. [[CrossRef](#)]

**Disclaimer/Publisher's Note:** The statements, opinions and data contained in all publications are solely those of the individual author(s) and contributor(s) and not of MDPI and/or the editor(s). MDPI and/or the editor(s) disclaim responsibility for any injury to people or property resulting from any ideas, methods, instructions or products referred to in the content.